PAK1 and PAK2 in the cell metabolism regulation

Tereza Kořánová, Lukáš Dvořáček, Dana Grebeňová, Pavla Röselová, Adam Obr, Kateřina Kuželová*

*corresponding author: kuzelova@uhkt.cz, ORCID ID: 0000-0002-9628-6255

Affiliation of all the authors: Institute of Hematology and Blood Transfusion, Dpt of Proteomics, U Nemocnice 1, 128 20 Prague 2, Czech Republic

Running title: PAK1 and PAK2 in the cell metabolism

Abstract

P21-activated kinases (PAK) regulate processes associated with cytoskeletal rearrangements, such as cell division, adhesion, and migration. Possible regulatory role of PAK in the cell metabolism is little explored, but increasing evidence suggests that a cell metabolic phenotype is related to cell interaction with the microenvironment. We analyzed the impact of PAK inhibition by small molecule inhibitors, small interfering RNA, or by gene knock-out on the rates of mitochondrial respiration and aerobic glycolysis. Pharmacological inhibition of PAK group I by IPA-3 induced a strong decrease of the both metabolic rates in adherent cancer cell lines, leukemia/lymphoma cell lines, and primary leukemia cells. The effect of FRAX597, which inhibits PAK kinase activity only, was moderate, indicating that PAK non-kinase functions are essential for the cell metabolism. Selective downregulation or deletion of PAK2 was associated with a shift towards oxidative phosphorylation. However, the overall metabolic capacity was not substantially reduced by PAK1 or PAK2 deletion, possibly due to partial redundancy in PAK1/PAK2 regulatory roles.

Keywords: cell metabolism, p21-activated kinase 1, p21-activated kinase 2, oxidative phosphorylation, glycolysis

Introduction

P21-activated kinases (PAK) participate in the regulation of virtually all processes associated with cytoskeletal rearrangements, such as cell migration, apoptosis, or cell division. PAK activity is often upregulated in cancer (Rane & Minden, 2019), and PAK are therefore considered as potential therapy target (Binder et al., 2019; Kanumuri et al., 2020; Senapedis, Crochiere, Baloglu, & Landesman, 2016). In relation to tumorigenesis, PAK are obviously involved in modulation of cell adhesion and migration properties, which are critical for metastasis formation. The epithelial-to-mesenchymal transition (EMT), which promotes cancer cell invasivity, was reported to be associated with changes in the cell metabolism, another hallmark of oncogenic cell transformation. In general, tumor cells often rely on aerobic glycolysis (so-called Warburg effect) to cover increased biosynthetic and energetic needs, as well as to maintain the redox state. Nevertheless, they keep the ability to switch among different metabolic phenotypes and to adapt to environmental changes (Kreuzaler, Panina, Segal, & Yuneva, 2020). Cell-cell and cell-matrix interactions have impact on the cell metabolic phenotype, at least in solid tumors (Sousa, Pereira, & Paredes, 2019). The oxidative phosphorylation prevents cell migration by generation of reactive oxygen species (ROS), which induce anoikis, a specific form of cell death caused by a loss of cell attachment (Lu, Tan, & Cai, 2015). In migrating cells, increased glycolysis is associated with deviation of intermediates to pentose phosphate pathway, which produces the major ROS scavenger, nicotineamide dinucleotide phosphate (NADPH), providing protection from ROS-induced toxic effects (Sousa et al., 2019). Vice versa, metabolites produced by aerobic glycolysis promote EMT and cell migration (Han et al., 2013).
Despite increasing evidence of interconnection between the cell metabolism and cell interaction with the microenvironment, little is known about possible role of PAK in regulation of metabolic processes. The human PAK protein family consists of two groups, each of them containing products of three different genes. The group I includes three serine/threonine kinases (PAK1 to PAK3) with nearly identical kinase domains, but at least partly different functions (Coniglio, Zavarella, & Symons, 2008; Grebenova et al., 2019; Kumar, Sanawar, Li, & Li, 2017). PAK3 expression is limited to a few cell types. PAK1 and PAK2 are found in the majority of cells, and some previous reports indicated their involvement in regulation of the cell metabolism (Fig. 1). PAK2 was proposed to mediate E-cadherin

signaling through activation of AMPK, a metabolic regulator promoting glucose uptake (Campbell, Salvi, O'Brien, Superfine, & DeMali, 2019). In muscle cells, insulin-induced glucose uptake is mediated by PAK1 (Tunduguru et al., 2014). PAK1 also enhances the function of phosphoglucomutase 1, an enzyme interconverting glucose-1-phosphate and glucose-6-phosphate (Gururaj, Barnes, Vadlamudi, & Kumar, 2004) On the other hand, PAK2 activity leads to decreased glucose uptake in neuronal cells (Varshney & Dey, 2016). Apart from glucose uptake and conversion, PAK2 is involved in a feedback loop activating the pyruvate kinase isoform PKM2, which supports pyruvate conversion to lactate (aerobic glycolysis) rather than the Krebs cycle supply (Cheng et al., 2018; Gupta et al., 2018). PAK1 activity is also connected to the kinase mTOR, which belongs to key metabolic regulators. However, the mTOR interactome is complex and PAK1 was reported to be both upstream and downstream from mTOR, suggesting possible feedback loops (Kim et al., 2020; Rouquette-Jazdanian et al., 2015).
Cell adhesion processes are somewhat different in leukemia cells, which do not form stable cell-matrix or cell-cell contact points. Nevertheless, they interact with stromal cells, as well as with extracellular matrix (ECM) proteins of the bone marrow, and these interactions have profound impact on their behavior. The adhesion structures of leukemia cells are more dynamic compared to those of adherent cells, they are usually not tightly connected to the actin cytoskeleton, but PAK group I regulate cell adhesion to ECM also in these cells (Kuželová et al., 2021). In addition, PAK are indispensable for leukemia cell survival, as their inhibition leads to rapid cell death (Kuzelova, Grebenova, Holoubek, Roselova, & Obr, 2014; Kuželová et al., 2021; Pandolfi et al., 2015). Similarly to solid tumors, leukemia cells often display a preference for aerobic glycolysis (Jiang & Nakada, 2016), and the metabolic phenotype has been proposed as prognostic parameter for clinical outcome in acute myeloid leukemia (Chen, W. L. et al., 2014; Herst, Howman, Neeson, Berridge, & Ritchie, 2011). In leukocytes, PAK1 was reported to inhibit glycolysis through binding to phosphoglycerate mutase B, which converts 3-phosphoglycerate to 2-phosphoglycerate (Shalom-Barak & Knaus, 2002).
The interconnection between adhesion and metabolic signaling together with the key role of PAK in regulation of cell adhesion and migration prompted us to analyze possible regulatory function of PAK group I in metabolic processes. In the present work, we modulated PAK activity in adherent and leukemia cells using several approaches: pharmacological inhibition of kinase or non-kinase PAK function, reduction of PAK transcript levels using siRNA, and gene knock-out. The induced changes in the rates of mitochondrial respiration (OCR) and lactate production (ECAR) were monitored using Seahorse XFp analyzer. The effect of inhibitors on glucose uptake was analyzed using a fluorescent derivative of 2-deoxyglucose, which was detected by flow cytometry.

Materials & methods

Cell lines and primary cells

HeLa, HEK293T, and HEL cells were obtained as a gift and authenticated using analysis of short tandem repeats, the results were compared with ATCC database. OCI-AML3, Karpas-299, and Jurkat cell lines were purchased from DSMZ (Germany). After receipt, the cells were shortly expanded and aliquots were cryopreserved for later use. The cell line MOLM-7 (not commercially available) was obtained from the laboratory of origin (Tsuji-Takayama et al., 1994). The majority of cell lines were cultured in RPMI-1640 medium with 10% fetal calf serum (FCS), 100 U/ml penicillin, and 100 µg/ml streptomycin at 37°C, in 5% CO_2 humidified atmosphere, except for HEK293T (DMEM medium) and OCI-AML3 (alpha-MEM medium, 20% FCS).
Primary cells from patients with acute myeloid leukemia were obtained from leukapheresis at diagnosis. All patients provided their written informed consent as to the use of their biological material for research purposes, in accordance with the Helsinki Declaration. The project was approved by the Ethics Committee of the Institute of Hematology, and all experiments were

performed in accordance with relevant guidelines and regulations. The leukapheretic products were diluted 20-fold in phosphate buffered saline (PBS) and the mononuclear cell fraction was then separated using Histopaque-1077 (Sigma, #H8889).

Cell transfection with siRNA

ON-TARGETplus siRNA (Dharmacon) targeting PAK1 (#L-003521) or PAK2 (#L-003597), in parallel with non-targeting control (#D-001810), were transfected using jetPRIME transfection reagent (Polyplus Transfection) following the manufacturer's instructions. The concentration range for siRNA was 100 to 150 nM (final concentration during transfection). The cells were then cultivated for 24 h without changing medium, harvested, and seeded into Seahorse plates for cell metabolism measurement or into Petri dishes for protein analysis by western-blotting.

Gene knock-out

To generate cells with PAK1 or PAK2 knock-out via non-homologous end-joining, we designed single guide RNA (sgRNA) sequences as follows ($(N)_{19\text{-}20}$NGG strand, 5´ to 3´)): PAK1 sgRNA – ATTTGATGTCTGAAGCAAGC, PAK2 sgRNA – CATGTCTGATAACGGAGAAC, HPRT1 sgRNA - AAGTAATTCACTTACAGTC. Cas9 enzyme and sgRNA were obtained from IDT (Alt-R® S.p. HiFi Cas9 Nuclease V3, Alt-R® CRISPR-Cas9 sgRNA). HeLa cells were transfected with the enzyme and with PAK1 or PAK2 sgRNA using nucleofection (4D-Nucleofector™ X Unit, Lonza). Due to low transfection efficiency in leukemia cell lines, OCI-AML3 cells were co-transfected with sgRNA targeting the hypoxanthine phosphoribosyltransferase 1 (HPRT1) gene. This allowed for enrichment of successfully transfected cells through resistance to 6-thioguanine (6-TG). Typical transfection reaction contained $4x10^5$ HeLa cells or $1x10^6$ OCI-AML3 cells, 500 pmol Cas9 enzyme, and 600 pmol sgRNA (2x 300 pmol in case of HPRT1 co-transfection). After transfection, HeLa cells were seeded in 6-well plates and grown according to experiment settings. OCI-AML3 cells were seeded in 6-well plates, 6-TG was added (10 µg/ml final concentration) after 3 days, and the cells were cultured for at least 10 days with regular changes of 6-TG containing media.

Inhibitors and antibodies

IPA-3 (#3622) and PIR3.5 (#4212) were purchased from Tocris Bioscience and dissolved in sterile dimethylsulfoxide (DMSO) to make 50 mM stock solutions. Working solutions were prepared by 10-fold dilution of the stock solution in 50 mM Tris, pH 8.0, immediately before use. FRAX597 (#6029) was purchased from Tocris Biosciences and dissolved in sterile DMSO to make 10 mM stock solution. Working solution was prepared by 10-fold dilution in cell culture medium. Dasatinib was obtained from Selleckchem (S1021), 200 µM stock solution was made in sterile DMSO. The following antibodies were used: PAK1 (Abcam, ab223849), PAK2 (Abcam, ab76293), PAK1 (phosphoS144)+PAK2 (phosphoS141)+PAK3 (phosphoS139) (Abcam, ab40795), β-actin (Sigma-Aldrich, A5441).

Cell metabolism measurement

The oxygen consumption rate (OCR) and the extracellular acidification rate (ECAR) were measured using the MitoStress Test kit (Agilent, #103010-100), following the manufacturer´s instructions. The last injection was supplemented with 2-deoxyglucose (2-DG, Sigma, D8375) to obtain ECAR background value due to non-glycolytic acidification. If not otherwise indicated, the final well concentrations were the following: oligomycin (OM) 1 µM, carbonyl cyanide-4 (trifluoromethoxy) phenylhydrazone (FCCP) 0.3 and 0.5 µM, rotenone/antimycin A 0.5 µM, 2-DG 50 mM.

In the experiments involving glycolytic stress, glucose (10 mM) and pyruvate (1 mM) were omitted from the Seahorse medium and the injections were the following: glucose 10 mM, OM 1 µM, FCCP 0.4 µM, rotenone/antimycin A 0.5 µM with 50 mM 2-DG. CellTak (Corning, #354240) was used to coat Seahorse XFp plates according to manufacturer´s instructions for all leukemia cells, as well as for HEK293T cells. HeLa (16,000 cells/well) or HEK293T (20,000 cells/well) were seeded in 80 µl culture medium and incubated overnight. The plate was then washed with Seahorse medium (Agilent #103676-100 or #103575-100, respectively), the cells were treated with inhibitors if appropriate and incubated for 1h at 37 °C, without CO_2. The control cells were treated with the solvent only. When IPA-3 and PIR3.5 were used for cell treatment, the plates were washed twice with Seahorse medium and analyzed using the Seahorse XFp apparatus (Agilent). Cells treated with FRAX597 or transfected cells were measured without washing. After measurement, the medium was aspirated, the plate was cryopreserved, and the cell amounts in the individual wells were assessed using CyQuant Cell Proliferation Assay Kit (Molecular Probes, #C7026). The records were normalized to the cell numbers and analyzed using the Wave software (Agilent). Leukemia cells (40,000 cells/well for cell lines, 150,000-200,000 cells/well for primary cells) were seeded in 50 µl Seahorse medium (Agilent #103676-100), shortly centrifuged (1 min, 200 g, gentle brake), incubated for 25 min at 37°C without CO_2 prior to addition of 130 µl medium, treated with inhibitors for 1h, and subjected to analysis.

Glucose uptake assay

Cells ($5x10^5$) were washed once in PBS, resuspended in 0.5 ml Seahorse medium with glutamine, without glucose, and treated with the inhibitors for 1h. A fluorescent derivative of 2-deoxyglucose (2-NBDG, Invitrogen, N13195) was added at 20 µM final concentration for further 30 min incubation at 37°C. Then, the cells were washed in cold PBS (300 g/4°C/5 min) and resuspended in 0.5 ml cold PBS, the samples were placed on ice, and 2-NBDG fluorescence was immediately analyzed using the FITC channel on a BD Fortessa flow cytometer. Propidium iodide (10 µg/ml final concentration) was added before measurement to exclude dead cells from the analysis, the cell debris was outgated in scattergrams. The mean fluorescence intensity (MFI) of control cell samples without 2-NBDG was used to determine the background, which was subtracted from the corresponding MFI of samples with 2-NBDG.

Western-blot

Adherent cells were washed once with ice-cold HBS (HEPES – buffered saline; 20 mM HEPES, 150 mM NaCl, pH 7.1) and scrapped into Pierce IP Lysis Buffer (#87787) with freshly added protease and phosphatase inhibitors. The suspension was then transferred to a centrifugation tube and incubated for 10 min at 4 °C. Cellular debris was removed by centrifugation (15,000 g/4 °C/15 min), the lysate was mixed 1:1 (v/v) with 2x Laemmli sample buffer and incubated for 5 min at 95 °C.
An equivalent of 20 µg total protein was resolved on 7.5% polyacrylamide gel (18×18 cm) and transferred to a nitrocellulose membrane. The membrane was blocked for 1h in 3% bovine serum albumin and incubated for 1h with the primary antibody in PBS with 0.1% Tween-20 (PBST), at room temperature. Thereafter, it was washed in PBST six times and incubated with the corresponding HRP-conjugated secondary antibody for 1h. The chemiluminiscence signal from Clarity Western ECL Substrate (BioRad, #170-5060) was detected and analyzed using G:BOX iChemi XT-4 (Syngene).

Statistical analyses

Statistical evaluation of experimental results was performed using the GraphPad Prism 7 software. The p-value limit for statistically significant differences between groups was set to 0.05.

Results

Study design

Mitochondrial respiration and aerobic glycolysis (lactate production) were analyzed using Seahorse XFp device, which monitors the oxygen consumption rate (OCR) in parallel with the extracellular acidification rate (ECAR). An example of Seahorse XFp record is shown in the Supplementary Fig. S1, which also depicts the basal and maximal metabolic rates. The standard Seahorse assay was performed in serum-free culture medium supplemented with glucose, pyruvate, and glutamine. After signal stabilization (4 cycles), three compounds were added in four injections: oligomycin (OM) inhibits the ATP synthase, the protonophore FCCP (two injections) dissipates the proton gradient across the mitochondrial membrane, and a mixture of rotenone with antimycin A and with 2-deoxyglucose (rot/A+2-DG) inhibits both the respiration chain and glycolysis, thereby giving the signal background to be deduced from both the basal and maximal metabolic rates. To determine the effect of PAK inhibition on the processes non-associated with glucose uptake and/or consumption, OCR was also measured in glucose-free and pyruvate-free medium. Under these conditions, ECAR values were very low and the cells mainly relied on the oxidative phosphorylation to produce energy. The amount and/or activity of PAK were modified using small molecule inhibitors, small interfering RNAs (siRNA), or CRISPR/Cas9 knock-out. The inhibitor IPA-3 binds to inactive PAK group I molecules and prevents conformational changes, which are necessary for PAK activation (Deacon et al., 2008). A structural isomer of IPA-3, called PIR3.5, displays no inhibitory activity towards PAK1 (Deacon et al., 2008), and is thus commonly used as a negative control compound to IPA-3. An alternative PAK inhibitor, FRAX597, binds to the ATP-binding site of kinase-active PAK molecules and prevents PAK kinase activity, but presumably does not directly interfere with non-kinase PAK functions (Licciulli et al., 2013). We have previously described the effects of these inhibitors on cell adhesion and viability in adherent HeLa and HEK293T human cancer cell lines (Grebenova et al., 2019) as well as in human leukemia cells (Kuželová et al., 2021). In the present work, we used the inhibitors at optimized concentrations regarding the efficiency and toxicity: 20 and 50 µM for IPA-3/PIR3.5, 2 and 10 µM for FRAX597. The efficiency of PAK silencing by siRNA or by gene knock-out was assessed by western-blotting using previously characterized antibodies against PAK1, PAK2, or the autophosphorylated site Ser144/141 of PAK1/PAK2 (Grebenova et al., 2019).

Effect of PAK inhibitors on the cell metabolism in adherent cells

HeLa or HEK293T cells were seeded into Seahorse plates and cultured for 24 h. The medium was replaced by the corresponding serum-free variant, and the cells were treated for 1h with inhibitors. Treatment with IPA-3 substantially reduced both OCR and ECAR (Fig. 2A). The effect of the control compound, PIR3.5, was always more moderate if any, and cell type-specific. In contrast to IPA-3, only limited changes in the cell metabolic rates were observed after FRAX597 treatment (Fig. 2B).

Effect of PAK inhibitors on the cell metabolism in leukemia cells

Leukemia cells were reported to be very sensitive to PAK inhibition (Kuzelova et al., 2014; Kuželová et al., 2021; Pandolfi et al., 2015), and treatment with IPA-3 induces cell death in the majority of leukemia cell lines. Accordingly, both OCR and ECAR were markedly reduced by 20 µM IPA-3 in all leukemia cell lines tested (Fig. 3A), except for MOLM-7, which have very low PAK1 level and high PAK2 level (Kuželová et al., 2021). Increasing IPA-3 dose to 50 µM was sufficient to achieve a marked decrease of OCR and ECAR also in this cell line (data not shown). In agreement with the findings in adherent cell models, inhibition of PAK kinase activity by FRAX597 had lower impact on the metabolic rates of leukemia cell lines compared to treatment with IPA-3 (Fig. 3B). Nevertheless, leukemia cell metabolic capacity was reduced by FRAX597 treatment. We also performed several experiments with primary cells from patients with acute myeloid leukemia (Supplementary Fig. S2).

As the signal from these cells was lower than that from cell lines, higher amount of cells (150 to 200 thousand per well) was required for Seahorse XFp measurement compared to the cell lines (40 thousand per well). On the other hand, we have shown previously that the efficiency of IPA-3 strongly depends on the cell density. Therefore, primary cell suspension at 3×10^5 cells/ml was pretreated with IPA-3 or PIR3.5 for 1h, the cells were washed and seeded into Seahorse plates for metabolic measurement. Under these conditions, the effects of 20 µM IPA-3 were not consistent (Fig. S2, panel A). However, the higher dose (50 µM) induced similar changes as in other cells, i.e. marked reduction of both OCR and ECAR (Fig. S2, panel B).

Effect of PAK inhibition on glucose uptake

Previous reports indicated PAK involvement in glucose uptake in some cell types, and limited glucose supply could explain the observed reduction of both OCR and ECAR in our model systems. We thus searched for possible involvement of PAK in the glucose uptake rate using a fluorescent derivative of 2-deoxyglucose (2-NBDG). Impact of IPA-3 pretreatment was cell type-specific, but no systematic reduction of the glucose uptake was found (Fig. 4A).

Effect of PAK inhibition under glycolytic stress conditions

PAK2 was shown to enhance cell preference for aerobic glycolysis rather than to the Krebs cycle and oxidative phosphorylation (Fig. 1). However, the observed large reduction of both OCR and ECAR upon PAK inhibition indicated that PAK might also be required for the mitochondrial respiration. We thus performed Seahorse measurement in the absence of glucose and pyruvate, thus limiting the use of the glycolytic pathway. Examples of records are provided in the Supplementary Figure S3. The measured OCR values from these experiments are summarized in Fig. 4B showing that the strong effect of IPA-3 was retained under these conditions.

Effect of siRNA-mediated PAK silencing

Small interfering RNAs (siRNA) were used to discriminate between PAK1 and PAK2 function in the cell metabolism. The efficiency of silencing was measured by western-blotting, examples are given in the Supplementary Fig. S4. As summarized in Fig. 5A, we observed some cross-effects at PAK protein levels: siRNA PAK1 reduced PAK2 protein level in HEK293T cells (left) and, conversely, siRNA PAK2 reduced PAK1 protein level in both HeLa and HEK293T (right). This might be due to mutual interaction and possibly to mutual regulation between PAK1 and PAK2 (Grebenova et al., 2019). HeLa cells have low PAK1 levels compared to HEK293T (Grebenova et al., 2019) Accordingly, PAK1 targeting by siRNA PAK1 was more efficient in HeLa cells (Fig. 5A, left).

Fig. 5B shows the results of individual Seahorse XFp experiments with cells treated with PAK1 or PAK2 siRNA (top) as well as the summary and statistical evaluation of these results (bottom). Both PAK1 and PAK2 siRNA reduced both OCR and ECAR, the effect of siRNA PAK2 being more pronounced on ECAR values. Treatment with siRNA resulted in a decrease of OCR also in the absence of glucose and pyruvate (Supplementary Fig. S5).

Effect of PAK1 knock-out

As an alternative method to specifically reduce PAK1 or PAK2 expression, we performed *PAK1/PAK2* gene knock-out (KO) in HeLa cells using CRISPR/Cas9 system. Western-blot analysis confirmed a substantial reduction of the respective PAK1/PAK2 protein levels (Fig. 6A). The impact of PAK KO on HeLa cell metabolic rates is shown in Fig. 6B. The overall metabolic activity of cells with PAK1 or PAK2 KO was not very different from that of the control cells (nucleofection without CRISPR modification). However, the metabolic phenotype was shifted towards glycolysis in KO PAK1, and towards oxidative phosphorylation in KO PAK2, in agreement with the results obtained using siRNA-mediated PAK targeting (cf Fig. 5B, lower right).

The transfection efficiency was much lower in leukemia cells and we thus used simultaneous HPRT KO to enrich OCI-AML3 cells with PAK1 KO through resistance to 6-thioguanine. Compared to cells with single HPRT KO, the cells with PAK1 KO had reduced OCR and increased ECAR (Fig. 6C), confirming the results obtained for HeLa cells. Unfortunately, attempts to reduce PAK2 expression by gene KO in OCI-AML3 cells were not successful, possibly because PAK2 is essential for leukemia cell survival.

Effect of dasatinib and PIR3.5 combination with FRAX597

As PAK1 is known to be an important downstream effector of c-Src in adherent cells, we have also looked for possible effect of Src kinase inhibition by dasatinib on the metabolic rates in HeLa and HEK293T cells. Supplementary Fig. S6 shows that neither OCR nor ECAR were reduced by 1h 100 nM dasatinib treatment.

Milder effect of FRAX597 compared to IPA-3 indicated that non-kinase activity of PAK is essential for the cell metabolism. However, as the control compoud PIR3.5 also affected the cell metabolism, IPA-3 might have unspecific effects, such as reactive oxygen species generation, which could act in synergy with inhibition of PAK kinase activity. To check for this possibility, we analyzed the effect of combined treatment with FRAX597 and PIR3.5. However, we detected no synergy between these two compounds (Supplementary Fig. S7).

Discussion

Our results suggest that PAK group I regulate the cell metabolism in a variety of cell types. Treatment with IPA-3, which is considered specific for PAK group I, rapidly inhibits both the cell respiration and the aerobic glycolysis in adherent cancer cell lines (Fig. 2A), in leukemia cell lines (Fig. 3A), as well as in primary leukemia cells (Supplementary Fig. S2). In primary cells, higher IPA-3 doses (50 µM instead of 20 µM) were needed to obtain consistent reduction of OCR and ECAR, but this might be due to different protocol used for the treatment because of the higher cell density required for Seahorse XFp measurement. Nevertheless, we cannot exclude lower sensitivity of primary cells to PAK inhibition in comparison with rapidly proliferating established cell lines.

IPA-3 could have additional unspecific effects, due e.g. to increased oxidative stress. Indeed, the control compound PIR3.5 also affected OCR and ECAR (Figs 2A, 3A, and S2). However, these unspecific effects were in general milder and varied according to cell type. For example, OCR reduction due to PIR3.5 treatment was compensated by increased glycolysis in HeLa cells (Fig. 2A). Similar effect was observed in one primary leukemia sample (Fig. S2B), but not in HEK293T cells, maybe because of the low reserve glycolytic capacity, as the maximal ECAR rate was roughly equal to the basal ECAR rate in the latter cell line. Although FRAX597 is less specific and might inhibit other kinases in addition to PAK group I (Licciulli et al., 2013), it had only limited effect on the metabolic rates (Figs 2B and 3B). PAK kinase activity is strongly inhibited by FRAX597 at the doses used (Grebenova et al., 2019; Kuželová et al., 2021), and we thus conclude that a non-kinase PAK function is essential for the cell metabolism. Possible synergy between targeting PAK kinase activity and unspecific effects, which might have explained the observed strong effect of IPA-3, was ruled out by analysis of combined treatment with FRAX597 and PIR3.5 (Supplementary Fig. S7).

Small interfering RNA targeting either PAK1 or PAK2 was used with the aim to discriminate between these PAK group I members. However, cross-effects were usually detected except for siRNA PAK1 in HeLa cells, where PAK2 level was not altered (Fig. 5A). Therefore, CRISPR/Cas9 knock-out of PAK1 or PAK2 gene was performed in HeLa cells to further confirm the observed differences between PAK1 and PAK2 (Fig. 6). Regardless of the method used, reduced PAK2 levels were associated with a shift of metabolic preferences towards oxidative phosphorylation in both HeLa and HEK293T cells (Figs 5B and 6B). PAK2 thus might be involved in pyruvate conversion to lactate, in agreement with previous

reports indicating that PAK2 favors the aerobic glycolysis to the detriment of the Krebs cycle and oxidative phosphorylation (Fig. 1). On the other hand, PAK1 targeting in HeLa or OCI-AML3 cells resulted in a more glycolytic phenotype (Figs 5B, 6B, and 6C). In HEK293T cells, PAK1 silencing using siRNA was less efficient and also induced a decrease in PAK2 amount (Fig. 5A). This cross-reduction of protein levels could be due to interaction between PAK1 and PAK2 proteins (Grebenova et al., 2019) rather than to cross-targeting of transcripts by siRNA.

Despite the described changes in the metabolic preferences, cells with PAK1 or PAK2 gene knock-out were viable and their overall metabolic activity was comparable with that of the control cells (Fig. 6). Whereas the acute inhibition of both PAK1 and PAK2 by IPA-3 led to strong reduction of the both metabolic rates (Figs 2A, 3A, and S2), none of the individual PAK isoforms is indispensable for the cell metabolism. It is thus possible that PAK1 and PAK2 regulatory roles are partly redundant. Indeed, PAK1 protein translated from the dominant PAK1 transcript isoform is similar to PAK2 (Grebenova et al., 2019). Alternatively, cells may be able to overcome the lack of PAK activity by activating other signaling pathways on a longer time scale. However, we were unable to derive viable HeLa cell clones with double PAK1 and PAK2 knock-out.

The majority of specific interaction points between PAK signaling and cell metabolic pathways reported to date were localized at the level of glucose uptake or glucose conversion to pyruvate (Fig. 1). In our model systems, PAK inhibition by IPA-3 did not consistently lower the glucose uptake (Fig. 4A). Furthermore, IPA-3 significantly lowered OCR even under glycolytic stress conditions, i.e. in the absence of glucose and pyruvate as fuels, both in adherent and leukemia cell lines (Fig. 4B). Thus, PAK targeting slows down the cell metabolism regardless of glucose availability, and further research is needed to describe the mechanisms of PAK regulatory function(s) in the cell metabolic pathways. It has already been shown that mTOR and PKM2, which belong to known metabolic regulators, are important mediators of PAK1 effects on glioma cell proliferation, migration, and drug resistance (Kim et al., 2020). On the other hand, inhibition of mTOR complex 1 with rapamycin or siRNA-mediated downregulation of raptor resulted in increased expression and activity of PAK1 in the lymphocytic cell line Jurkat (Rouquette-Jazdanian et al., 2015). Reduced expression of rictor, which forms part of mTOR complex 2, correlated with increased PAK1 activity in macrophages treated with fingolimod (Chen, W., Ghobrial, Li, & Kloc, 2018). In contrast, higher PAK1 activity resulting from mTOR activation was described in prostate cancer cells (Wang et al., 2017).

Conclusions

In conclusion, our results show that PAK group I are involved in regulation of both mitochondrial respiration and aerobic glycolysis. Pharmacological inhibition of PAK group I blocks the cell metabolism, the effect being mainly mediated by inhibition of PAK non-kinase function(s). Although the roles of PAK1 and PAK2 are probably partly redundant, PAK2 activity is specifically associated with a shift of cell metabolic preferences towards glycolysis. This is in agreement with a recent report indicating that PAK2 stimulates the activity of the cancer-specific isoform of pyruvate kinase, PKM2, which directs the cell metabolism to aerobic glycolysis (Gupta et al., 2018). An important yet undescribed crosstalk between PAK signaling and metabolic pathways seems to be situated within the Krebs cycle and/or within mitochondrial respiration.

Acknowledgement

The work was financially supported by the European Regional Development Fund, by the state budget of the Czech Republic (project AIIHHP: CZ.02.1.01/0.0/0.0/16_025/0007428, OP RDE, Ministry of Education, Youth and Sports), and by the Ministry of Health of the Czech Republic (project for conceptual development of the research organization No 00023736). The authors wish to thank M.Voráčová for expert technical assistance.

References

Binder, P., Wang, S., Radu, M., Zin, M., Collins, L., Khan, S., . . . Liu, W. (2019). Pak2 as a Novel Therapeutic Target for Cardioprotective Endoplasmic Reticulum Stress Response. *Circulation Research, 124*(5), 696-711. 10.1161/CIRCRESAHA.118.312829 [doi]

Campbell, H. K., Salvi, A. M., O'Brien, T., Superfine, R., & DeMali, K. A. (2019). PAK2 links cell survival to mechanotransduction and metabolism. *The Journal of Cell Biology, 218*(6), 1958-1971. 10.1083/jcb.201807152 [doi]

Chen, W. L., Wang, J. H., Zhao, A. H., Xu, X., Wang, Y. H., Chen, T. L., . . . Jia, W. (2014). A distinct glucose metabolism signature of acute myeloid leukemia with prognostic value. *Blood, 124*(10), 1645-1654. 10.1182/blood-2014-02-554204 [doi]

Chen, W., Ghobrial, R. M., Li, X. C., & Kloc, M. (2018). Inhibition of RhoA and mTORC2/Rictor by Fingolimod (FTY720) induces p21-activated kinase 1, PAK-1 and amplifies podosomes in mouse peritoneal macrophages. *Immunobiology, 223*(11), 634-647. S0171-2985(18)30046-9 [pii]

Cheng, T. Y., Yang, Y. C., Wang, H. P., Tien, Y. W., Shun, C. T., Huang, H. Y., . . . Hua, K. T. (2018). Pyruvate kinase M2 promotes pancreatic ductal adenocarcinoma invasion and metastasis through phosphorylation and stabilization of PAK2 protein. *Oncogene, 37*(13), 1730-1742. 10.1038/s41388-017-0086-y [doi]

Coniglio, S. J., Zavarella, S., & Symons, M. H. (2008). *Pak1 and Pak2 mediate tumor cell invasion through distinct signaling mechanisms*. United States:10.1128/MCB.01532-07

Deacon, S. W., Beeser, A., Fukui, J. A., Rennefahrt, U. E., Myers, C., Chernoff, J., & Peterson, J. R. (2008). *An isoform-selective, small-molecule inhibitor targets the autoregulatory mechanism of p21-activated kinase*. England:10.1016/j.chembiol.2008.03.005

Grebenova, D., Holoubek, A., Roselova, P., Obr, A., Brodska, B., & Kuzelova, K. (2019). *PAK1, PAK1Delta15, and PAK2: similarities, differences and mutual interactions*. England:10.1038/s41598-019-53665-6 [doi]

Gupta, A., Ajith, A., Singh, S., Panday, R. K., Samaiya, A., & Shukla, S. (2018). *PAK2-c-Myc-PKM2 axis plays an essential role in head and neck oncogenesis via regulating Warburg effect*. England:10.1038/s41419-018-0887-0 [doi]

Gururaj, A., Barnes, C. J., Vadlamudi, R. K., & Kumar, R. (2004). Regulation of phosphoglucomutase 1 phosphorylation and activity by a signaling kinase. *Oncogene, 23*(49), 8118-8127. 1207969 [pii]

Han, T., Kang, D., Ji, D., Wang, X., Zhan, W., Fu, M., . . . Wang, J. B. (2013). How does cancer cell metabolism affect tumor migration and invasion? *Cell Adhesion & Migration, 7*(5), 395-403. 10.4161/cam.26345 [doi]

Herst, P. M., Howman, R. A., Neeson, P. J., Berridge, M. V., & Ritchie, D. S. (2011). The level of glycolytic metabolism in acute myeloid leukemia blasts at diagnosis is prognostic for clinical outcome. *Journal of Leukocyte Biology, 89*(1), 51-55. 10.1189/jlb.0710417 [doi]

Jiang, Y., & Nakada, D. (2016). Cell intrinsic and extrinsic regulation of leukemia cell metabolism. *International Journal of Hematology, 103*(6), 607-616. 10.1007/s12185-016-1958-6 [doi]

Kanumuri, R., Saravanan, R., Pavithra, V., Sundaram, S., Rayala, S. K., & Venkatraman, G. (2020). Current trends and opportunities in targeting p21 activated kinase-1(PAK1) for therapeutic management of breast cancers. *Gene, 760*, 144991. S0378-1119(20)30660-0 [pii]

Kim, J. H., Seo, Y., Jo, M., Jeon, H., Kim, Y. S., Kim, E. J., . . . Suk, K. (2020). Interrogation of kinase genetic interactions provides a global view of PAK1-mediated signal transduction pathways. *The Journal of Biological Chemistry, 295*(50), 16906-16919. S0021-9258(17)50587-6 [pii]

Kreuzaler, P., Panina, Y., Segal, J., & Yuneva, M. (2020). Adapt and conquer: Metabolic flexibility in cancer growth, invasion and evasion. *Molecular Metabolism, 33*, 83-101. S2212-8778(19)30906-8 [pii]

Kumar, R., Sanawar, R., Li, X., & Li, F. (2017). *Structure, biochemistry, and biology of PAK kinases*. Netherlands: Elsevier B.V.S0378-1119(16)30981-7 [pii]

Kuzelova, K., Grebenova, D., Holoubek, A., Roselova, P., & Obr, A. (2014). *Group I PAK inhibitor IPA-3 induces cell death and affects cell adhesivity to fibronectin in human hematopoietic cells*. United States:10.1371/journal.pone.0092560 [doi]

Kuželová, K., Obr, A., Röselová, P., Grebeňová, D., Otevřelová, P., Brodská, B., & Holoubek, A. (2021). Group I p21-activated kinases in leukemia cell adhesion to fibronectin. *Cell Adhesion & Migration, 15*(1), 18-36. 10.1080/19336918.2021.1872760 [doi]

Licciulli, S., Maksimoska, J., Zhou, C., Troutman, S., Kota, S., Liu, Q., . . . Kissil, J. L. (2013). *FRAX597, a small molecule inhibitor of the p21-activated kinases, inhibits tumorigenesis of neurofibromatosis type 2 (NF2)-associated Schwannomas*. United States:10.1074/jbc.M113.510933 [doi]

Lu, J., Tan, M., & Cai, Q. (2015). The Warburg effect in tumor progression: mitochondrial oxidative metabolism as an anti-metastasis mechanism. *Cancer Letters, 356*(2 Pt A), 156-164. S0304-3835(14)00207-9 [pii]

Pandolfi, A., Stanley, R. F., Yu, Y., Bartholdy, B., Pendurti, G., Gritsman, K., . . . Steidl, U. (2015). *PAK1 is a therapeutic target in acute myeloid leukemia and myelodysplastic syndrome*. United States: by The American Society of Hematology.10.1182/blood-2014-12-618801 [doi]

Rane, C. K., & Minden, A. (2019). P21 activated kinase signaling in cancer. *Seminars in Cancer Biology, 54*, 40-49. S1044-579X(17)30249-3 [pii]

Rouquette-Jazdanian, A. K., Kortum, R. L., Li, W., Merrill, R. K., Nguyen, P. H., Samelson, L. E., & Sommers, C. L. (2015). miR-155 Controls Lymphoproliferation in LAT Mutant Mice by Restraining T-Cell Apoptosis via SHIP-1/mTOR and PAK1/FOXO3/BIM Pathways. *PloS One, 10*(6), e0131823. 10.1371/journal.pone.0131823 [doi]

Senapedis, W., Crochiere, M., Baloglu, E., & Landesman, Y. (2016). *Therapeutic Potential of Targeting PAK Signaling*. Netherlands:ACAMC-EPUB-68116 [pii]

Shalom-Barak, T., & Knaus, U. G. (2002). *A p21-activated kinase-controlled metabolic switch up-regulates phagocyte NADPH oxidase*. United States:10.1074/jbc.M206650200 [doi]

Sousa, B., Pereira, J., & Paredes, J. (2019). The Crosstalk Between Cell Adhesion and Cancer Metabolism. *International Journal of Molecular Sciences, 20*(8), 1933. doi: 10.3390/ijms20081933. 10.3390/ijms20081933 [doi]

Tsuji-Takayama, K., Kamiya, T., Nakamura, S., Matsuo, Y., Adachi, T., Tsubota, T., . . . Minowada, J. (1994). *Establishment of multiple leukemia cell lines with diverse myeloid and/or megakaryoblastoid characteristics from a single Ph1 positive chronic myelogenous leukemia blood sample*. JAPAN:

Tunduguru, R., Chiu, T. T., Ramalingam, L., Elmendorf, J. S., Klip, A., & Thurmond, D. C. (2014). Signaling of the p21-activated kinase (PAK1) coordinates insulin-stimulated actin remodeling

and glucose uptake in skeletal muscle cells. *Biochemical Pharmacology, 92*(2), 380-388. https://doi.org/10.1016/j.bcp.2014.08.033

Varshney, P., & Dey, C. S. (2016). P21-activated kinase 2 (PAK2) regulates glucose uptake and insulin sensitivity in neuronal cells. *Molecular and Cellular Endocrinology, 429*, 50-61. S0303-7207(16)30092-2 [pii]

Wang, Z., Jia, G., Li, Y., Liu, J., Luo, J., Zhang, J., . . . Chen, G. (2017). Clinicopathological signature of p21-activated kinase 1 in prostate cancer and its regulation of proliferation and autophagy via the mTOR signaling pathway. *Oncotarget, 8*(14), 22563-22580. 10.18632/oncotarget.15124 [doi]

Legend to Figures

Figure 1: ***PAK involvement in regulation of metabolic pathways.***
The scheme illustrates previously reported interaction points between PAK signaling and the cell metabolism. In the present work, we analyzed the effect of PAK group I inhibition on the rates of oxidative phosphorylation (OCR) and of lactate production (ECAR) in cancer/leukemia cell lines.

Figure 2: ***Effect of inhibitors on metabolic rates in adherent cells*****.**
Adherent HEK293T (left) or HeLa (right) cells were treated with inhibitors in duplicates and incubated for 1h at 37°C without CO_2 prior to metabolic measurement. The oxygen consumption rate (OCR) and the extracellular acidification rate (ECAR) were determined from Seahorse XFp records as shown in the Supplementary Fig. S1. The records were normalized to the cell numbers, the duplicates were averaged, and the rates were expressed as relative to the corresponding untreated controls. The graphs show the means and standard deviations of basal and maximal metabolic rates obtained from repeated experiments. Differences between treated samples and untreated controls were evaluated using standard paired Student t-test. * $p < 0.05$, ** $p < 0.01$, *** $p < 0.001$, **** $p < 0.0001$. A. Effect of IPA-3 (red bars) and PIR3.5 (green bars). Three to seven independent experiments were performed for each cell line and for each inhibitor concentration (20 or 50 µM as indicated). B. Effect of FRAX597 at 2 µM (blue bars) or 10 µM (magenta) concentration. Four independent experiments were performed for each cell line.

Figure 3: ***Effect of inhibitors on metabolic rates in leukemia cell lines***
Cells (40.000 per well) were seeded into CellTak-coated wells and incubated for 25 min prior to 1h treatment with inhibitors. The graphs show the means and standard deviations of basal (left) and maximal (right) metabolic rates from repeated experiments. A. Effect of 20 µM IPA-3 (red bars) or PIR3.5 (green bars). Three independent experiments were performed for MOLM-7 cells, two experiments for the other cell lines. B. Effect of FRAX597 at 2 µM (blue bars) or 10 µM (magenta) concentration. Three independent experiments were performed for each cell line except for MOLM-7 cells (two experiments).

Figure 4: ***Effect of IPA-3 on glucose uptake and on cell respiration under glycolytic stress***
A. The cells were seeded in glucose/pyruvate-free medium and treated with 20 µM IPA-3 or PIR3.5 for 1h prior to addition of 20 µM 2-NBDG. After further 30 min incubation, the cells were washed and the amount of accumulated 2-NBDG was determined by flow cytometry. The background mean fluorescence intensity (MFI) was obtained from control tubes without 2-NBDG and subtracted. MFI from treated samples were expressed as relative to the corresponding untreated controls, the bars represent the means and standard deviations from three independent experiments for each cell line. B. Basal metabolic rates were measured in the absence of glucose and pyruvate. ECAR values were very low under these conditions (see examples of Seahorse records in the Supplementary Fig. S3). The cells were seeded in glucose/pyruvate-free medium and incubated for 1h in the presence of 20 µM IPA-3 or PIR3.5 prior to measurement. The graph represents the means and standard deviations from three independent experiments for each cell line, the difference between the treated samples and the corresponding controls were evaluated using standard paired Student t-test. * $p < 0.05$, ** $p < 0.01$

Figure 5: ***Effect of siRNA targeting PAK1/PAK2***
The cells were transfected with non-targeting (NT), PAK1, or PAK2 siRNA and cultured for 24 h under standard conditions. Then, they were harvested, aliquots were seeded into microtitration plates in triplicates (NT siRNA and PAK1/PAK2 siRNA) and cultured for further 24 h prior to analysis on

Seahorse XFp. The remaining cells were further cultured for 24h in Petri dishes and used to check PAK1/PAK2 expression level and PAK phosphorylation at Ser144/141 by western-blotting. A. Reduction of PAK levels by siRNA. Western-blot band intensity values were expressed as relative to the corresponding NT siRNA controls. The labeling of individual PAK1 bands is shown in the Supplementary Figure S4. The graphs show mean values and standard deviations from three independent experiments for HeLa cell line and from three, resp. six experiments for HEK293T transfected with siRNA PAK1, resp. PAK2. In HEK293T cells, cross-effects of PAK1 siRNA on PAK2 level and of PAK2 siRNA on PAK1 p-band 3 were statistically significant (* $p < 0.05$).
B. The measured OCR and ECAR values were corrected for differences in cell numbers, the triplicates were averaged, and the rates were expressed as relative to the corresponding NT siRNA control. Top: correlation of changes in OCR and ECAR in individual experiments. Bottom: The graphs show the means and standard deviations of metabolic rates obtained from repeated experiments. The differences between samples transfected with PAK siRNA and the corresponding NT controls were evaluated using standard paired Student t-test. * $p < 0.05$, ** $p < 0.01$, *** $p < 0.001$, **** $p < 0.0001$.

Figure 6: ***Effects of CRISPR/Cas9 PAK knock-out***
A. HeLa cells were subjected to CRISPR/Cas9 knock-out (KO) of PAK1 or PAK2, and PAK protein levels were checked by western-blot 3 to 11 days later. The panel shows representative western-blots and a summary of relative band intensities from repeated experiments. B. Metabolic rates of HeLa cells with PAK1 or PAK2 KO were measured using Seahorse XFp and expressed as relative to the values from control cells (empty nucleofection). The bars show the means and standard deviations from five experiments with PAK1 KO and from eight experiments with PAK2 KO. C. In OCI-AML3 cells, HPRT gene was targeted simultaneously with PAK1 by CRISPR/Cas9 system, and the modified cell population was enriched through 6-thioguanine selection. Metabolic rates were compared between cells with double PAK1+HPRT KO and cells with single HPRT KO. The bars show the means and standard deviations from four experiments.

Figure1

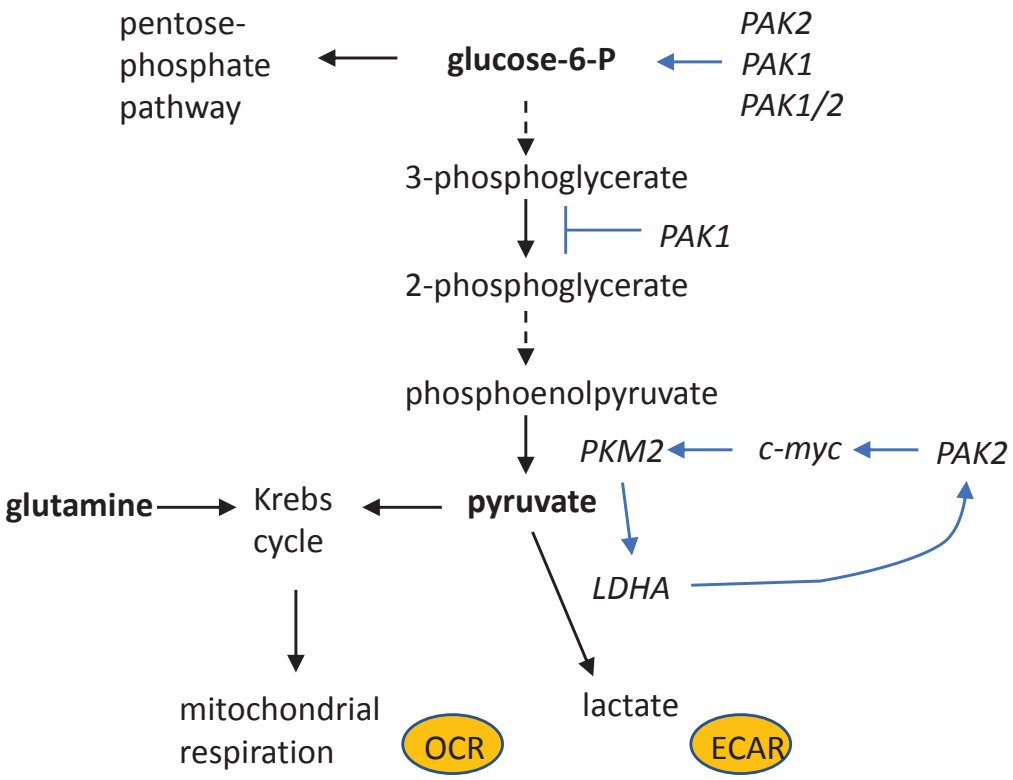
pentose-
phosphate
pathway
glucose-6-P
PAK2
PAK1
PAK1/2
3-phosphoglycerate
PAK1
2-phosphoglycerate
phosphoenolpyruvate
PKM2
c-myc
PAK2
glutamine
Krebs
cycle
pyruvate
LDHA
mitochondrial
respiration
OCR
lactate
ECAR

Figure 2

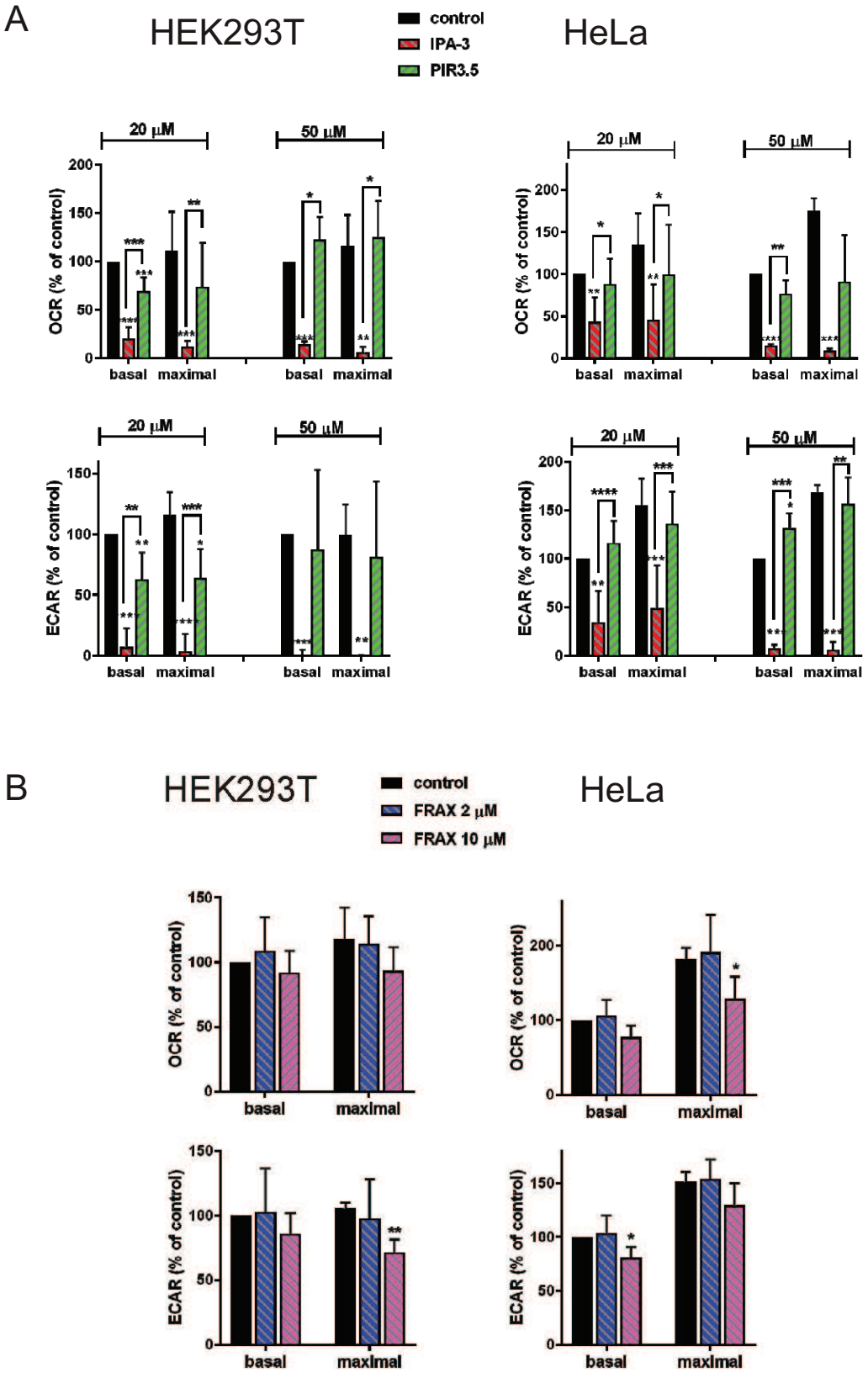
A
HEK293T
control
IPA-3
PIR3.5
HeLa
20 μM
50 μM
OCR (% of control)
ECAR (% of control)
basal
maximal
B
HEK293T
control
FRAX 2 μM
FRAX 10 μM
HeLa
OCR (% of control)
ECAR (% of control)
basal
maximal

Figure 3

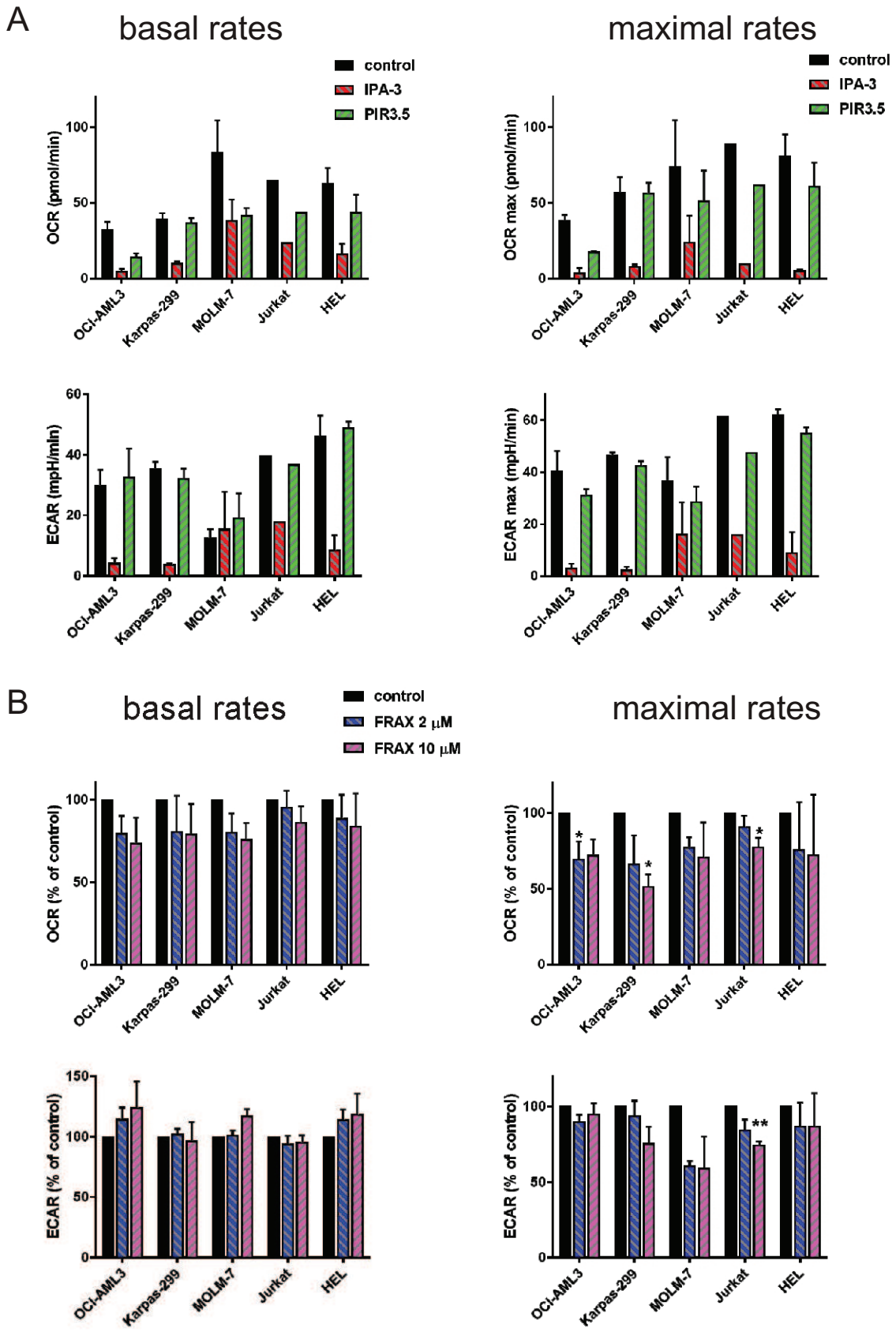
A
basal rates
maximal rates
control
IPA-3
PIR3.5
OCR (pmol/min)
OCR max (pmol/min)
ECAR (mpH/min)
ECAR max (mpH/min)
OCI-AML3
Karpas-299
MOLM-7
Jurkat
HEL
B
basal rates
maximal rates
control
FRAX 2 μM
FRAX 10 μM
OCR (% of control)
ECAR (% of control)
*
**

Figure 4

A

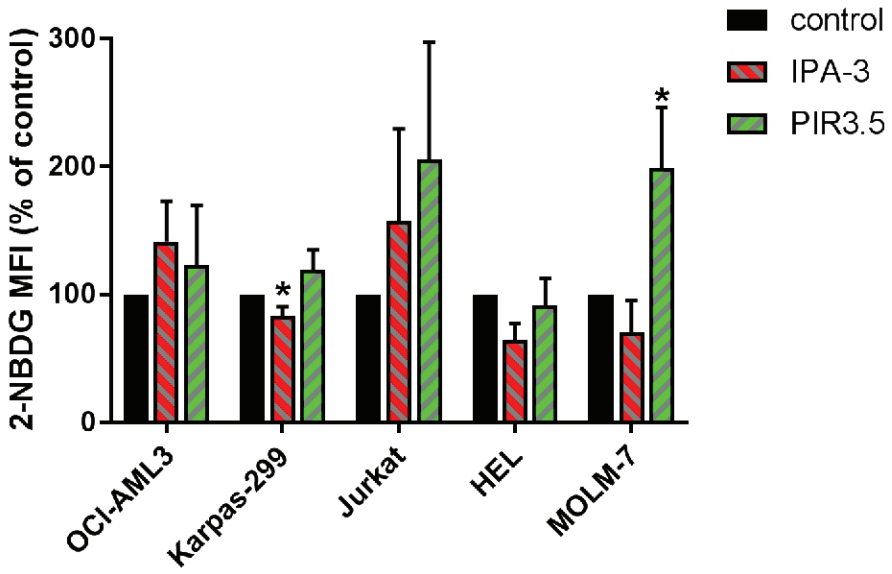
control
IPA-3
PIR3.5
2-NBDG MFI (% of control)
300
200
100
0
*
*
OCI-AML3
Karpas-299
Jurkat
HEL
MOLM-7

B

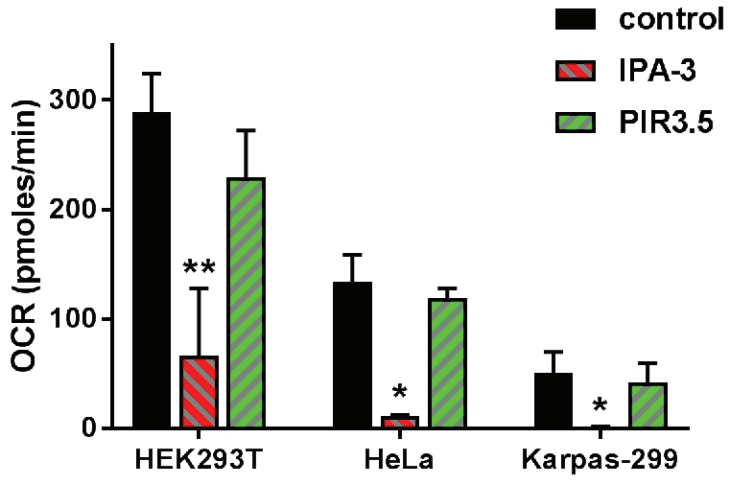
control
IPA-3
PIR3.5
OCR (pmoles/min)
300
200
100
0
**
*
*
HEK293T
HeLa
Karpas-299

Figure 5

A

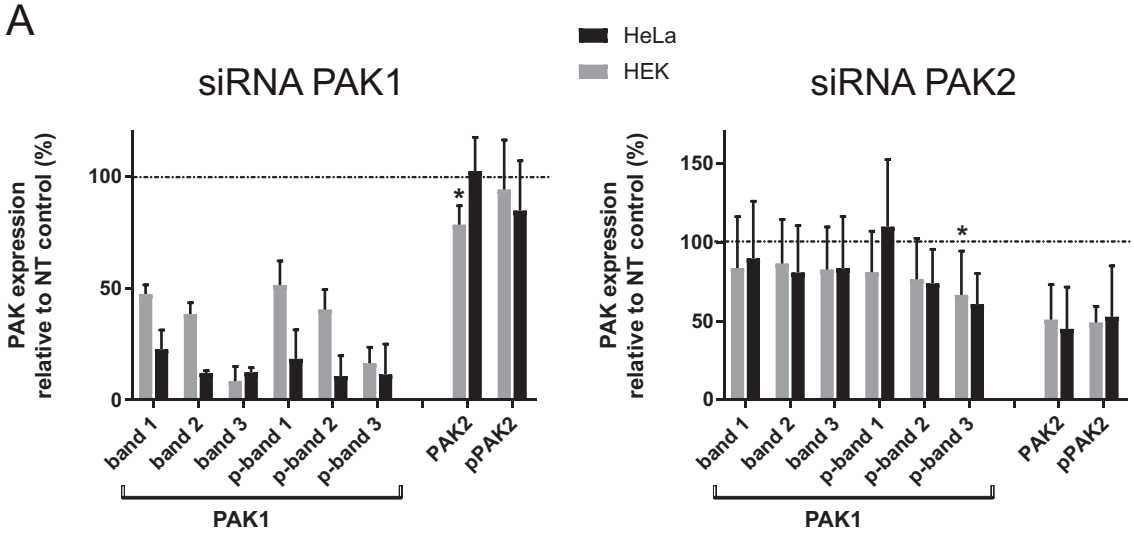
HeLa
HEK
siRNA PAK1
siRNA PAK2
PAK expression relative to NT control (%)
band 1
band 2
band 3
p-band 1
p-band 2
p-band 3
PAK2
pPAK2
PAK1

B

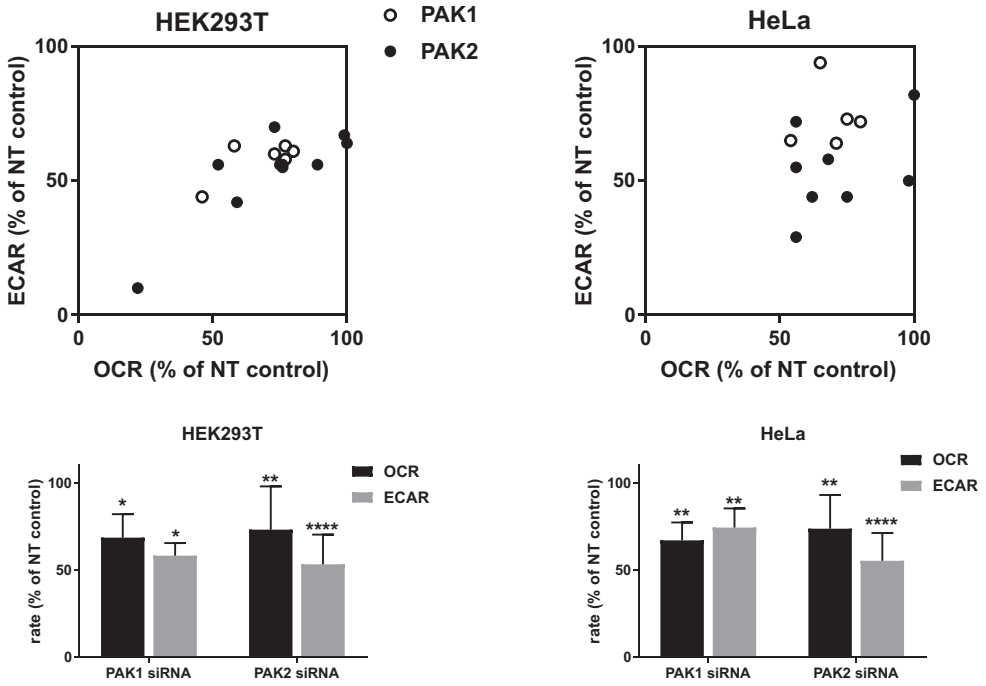
HEK293T
HeLa
PAK1
PAK2
ECAR (% of NT control)
OCR (% of NT control)
OCR
ECAR
rate (% of NT control)
PAK1 siRNA
PAK2 siRNA

Figure 6

A

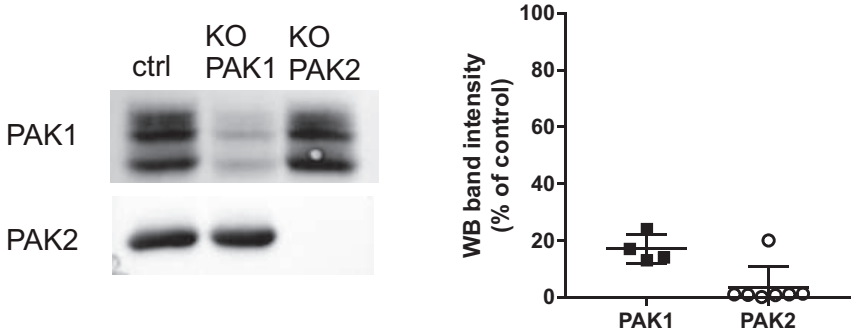
ctrl
KO PAK1
KO PAK2
PAK1
PAK2
WB band intensity (% of control)
100
80
60
40
20
0
PAK1
PAK2

B

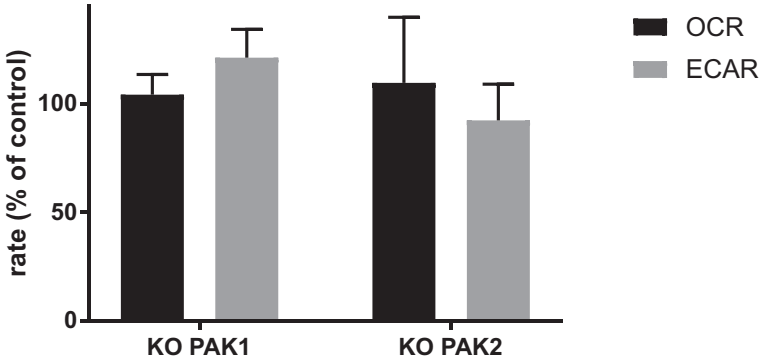
rate (% of control)
100
50
0
KO PAK1
KO PAK2
OCR
ECAR

C

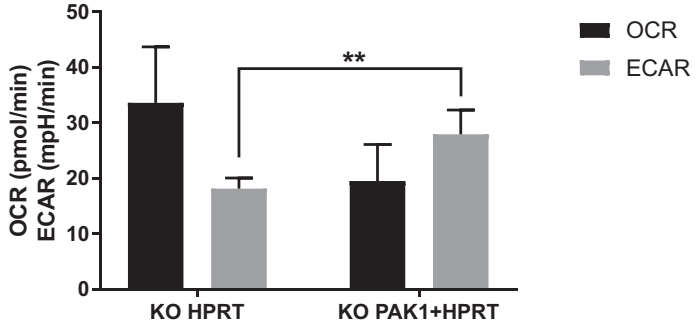
OCR (pmol/min)
ECAR (mpH/min)
50
40
30
20
10
0
**
KO HPRT
KO PAK1+HPRT
OCR
ECAR